

## FE analysis for radial spread behavior in three-roll cross rolling with small-hole and deep-groove ring

QIAN Dong-sheng<sup>1</sup>, HUA Lin<sup>1,2</sup>, DENG Jia-dong<sup>1</sup>

1. School of Materials Science and Engineering, Wuhan University of Technology, Wuhan 430070, China;

2. Hubei Key Laboratory of Advanced Technology of Automotive Parts,  
Wuhan University of Technology, Wuhan 430070, China;

Received 28 August 2012; accepted 25 October 2012

**Abstract:** To better understand the radial spread behavior and propose the effective control method, the FE analysis for radial spread in three-roll cross rolling (TRCR) was carried out using ABAQUS\Explicit procedure. The evolution and distribution laws of radial spread were studied, and the effects of four key forming parameters on the radial spread were investigated. The results obtained show that radial spread of the central region firstly increases, then decreases, and that of the upper or lower region always increases in TRCR process. The radial spread distribution is symmetrical about the axial centre after TRCR, it decreases from the upper and lower regions to the central region. A larger feed velocity or smaller rotational speed contributes to the larger average radial spread and more unevenness of inner surface, a larger friction coefficient or smaller initial blank temperature contributes to the smaller average radial spread and more unevenness of inner surface. The results can provide scientific basis for radial spread control and reasonable parameter design.

**Key words:** three-roll cross rolling; small-hole and deep-groove ring; radial spread; finite element analysis; rotary forming; plastic deformation

### 1 Introduction

Some mechanical ring parts in engineering machineries like duplicate gears and double-side flanges, have the common geometrical character of small hole, thick wall and deep groove on the surface, which are described as small-hole and deep-groove rings, as shown in Fig. 1. At present, this kind of ring is traditionally manufactured by forging and cutting. Hammer forging or die forging is adopted to preform the ring blank with

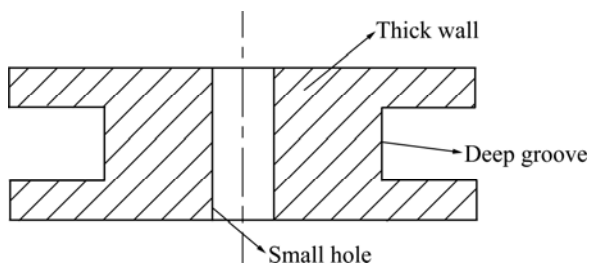


**Fig. 1** Cross-section of small-hole and deep-groove ring

simple cross-section, and cutting is used to process the ring groove. For this traditional technology, the forging has high energy consumption and low forming accurate; the great cutting not only consumes much materials and time, but also cuts off the metal flow line, thus results in the high material consumption, low productivity and poor quality.

Three-roll cross rolling (TRCR) is a new advanced rotary forming technology to manufacture the rotary cake parts and small-hole and deep groove rings. Its forming principle is shown in Fig. 2. In its forming process, the main roll makes active rotation and downward feed motion; the left and right passive rolls are idle roll, which make passive rotation under the driving of ring blank; the ring blank repeatedly enters into the rolling pass constructed by the three rolls, in which its material flows inversely to fill the roll cavities under the extrusion of rolls, under the accumulation of the multi-rotary deformation, the deep groove is formed and the ring is obtained finally.

Up to now, the researches for TRCR are very few,

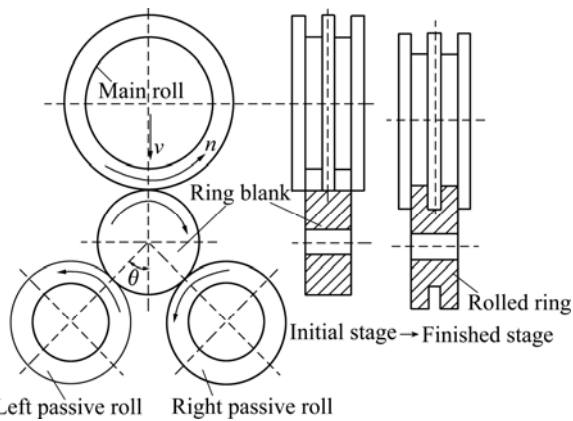


**Fig. 2** Forming principle of TRCR with small-hole and deep-groove ring

and many studies are being carried out in progress. ZHOU et al [1,2] made a first study on FE modeling and simulation for TRCR with cake parts, which described the key modeling techniques and developed a valid 3D coupled thermo-mechanical model based on ABAQUS/Explicit procedure, and researched the effects of key parameters on the deformation behaviors in the forming process. MA et al [3] afterwards performed the FE analysis work on TRCR with small-hole and deep-groove ring, and investigated the evolution and distribution laws of stain, temperature and force in the rolling process using ABAQUS/Explicit procedure. Additionally, this study shows that the inner surface of ring will produce a special deformation in the rolling process, as shown in Fig. 3, which is described as radial spread of inner surface. It can be seen that this radial spread is harmful for TRCR, as it obviously decreases the dimension accuracy of rolled ring, thus increases the material and time consumption of the following cutting. So, it is necessary to study the radial spread behavior in order to develop the application of this new plastic forming technology.

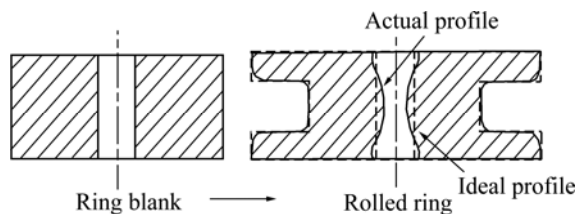


**Fig. 3** Radial spread of inner surface in TRCR with small-hole and deep-groove ring

As a rotary forming technology, TRCR process is a rapid time-variant process with complex thermo and mechanical deformation behavior and coupled multi-parameter effect, the traditional analytical methods based on some assumptions cannot accurately reveal its deformation laws, while the experimental method has expensive cost on equipment, materials and time. FE

simulation is an efficient and effective method, as it can intensively understand the deformation mechanism, directly display the forming defects and quickly optimize the important process parameters with the inexpensive cost [4]. It is regarded as a preferred research method for rotary forming technologies recently, especially for hot ring rolling process which is similar to TRCR process. WANG et al [5,6] developed a 3D coupled thermo-mechanical model for hot ring rolling process, and compared the evolution laws of stress and stain fields in hot rolling of titanium alloy large rings with different sizes using ABAQUS/Explicit procedure. KIM et al [7] simulated the hot rolling process of large profile ring with outer groove under MSC.SuperForm environment. SUN et al [8] performed the thermo-mechanical analysis for hot rolling process with alloy steel ring based on DEFORM 3D software. WANG et al [9,10] performed the virtual hot ring rolling process with LS\_DYNA code, and described the key modeling technologies and optimized the forming parameters. HUA et al [11] established the stiffness condition of hot radial-axial ring rolling process based on FEM. ZHOU et al [12,13] developed a 3D coupled thermo-mechanical FE model for hot radial-axial ring rolling process using ABAQUS/Explicit procedure, and investigated the deformation behaviors during the forming process. GUO et al [14] determined the steady forming condition of hot radial-axial ring rolling process based on FEA with ABAQUS/Explicit procedure.

In this work, FE simulation is carried out under ABAQUS/Explicit environment to analyze the radial spread behavior, explore its evolution rule and influence factors, and supply the effective scientific basis for technology design.

## 2 3D FE modelling

TRCR process has many similar characteristics to hot ring rolling process, as they are both rotary forming processes for ring parts. Many researches of FE modeling and simulation for hot ring rolling process have been carried out as mentioned above, the reliabilities of related modeling methods and techniques were experimentally testified. Referring to these research results, the study on TRCR FE modeling has been carried out in our previous work [1,3], in which an effective 3D coupled thermo-mechanical model was developed and verified, and the key modeling technologies were introduced. Then, based on the previous work, a 3D coupled thermo-mechanical FE model for TRCR with one small-hole and deep-groove ring was established using ABAQUS/Explicit procedure, which can be believed reliable, as shown in Fig. 4. The main parameters for the FE model are shown in Table 1.

**Table 1** Parameters for FE model

Outer radius of ring, $R/mm$	Inner radius of ring, $r/mm$	Deepness of groove, $D_g/mm$	Height of groove, $H_g/mm$	Height of ring, $H/mm$
54.5	16.5	24.5	20	56
Outer radius of blank, $R_0/mm$	Inner radius of blank, $r_0/mm$	Height of blank, $H_0/mm$	Radius of main roll, $R_m/mm$	Radius of passive roll, $R_{pl}, R_{pr}/mm$
93.08	16.5	56	230	130
Positon angle of passive roll, $\theta/(^\circ)$	Feed speed of main roll, $v/(mm \cdot s^{-1})$	Rotation speed of main roll, $n/(rad \cdot s^{-1})$	Temperature of blank/ $^\circ C$	Temperature of roll/ $^\circ C$
45	2.5	5	1200	80
Temperature of environment/ $^\circ C$	Friction coefficient	Heat transmission coefficient/ $(N \cdot s^{-1} \cdot mm^{-1} \cdot ^\circ C^{-1})$	Heat convection coefficient/ $(N \cdot s^{-1} \cdot mm^{-1} \cdot ^\circ C^{-1})$	Heat radiation coefficient/ $(N \cdot s^{-1} \cdot mm^{-1} \cdot ^\circ C^{-4})$
20	0.3	10	0.02	0.7

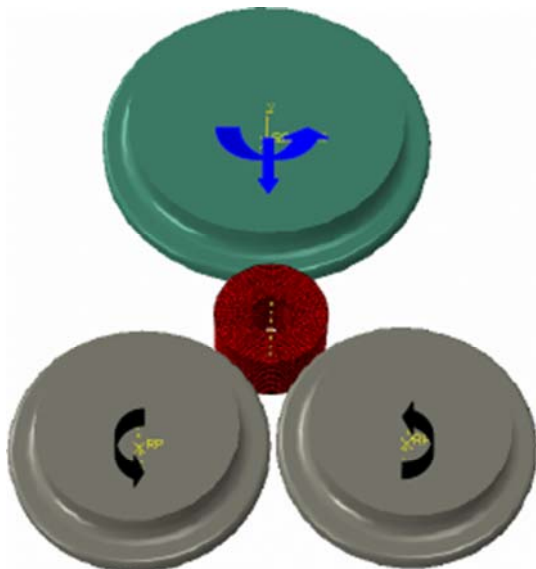


**Fig. 4** 3D FE model for TRCR with small-hole and deep-groove ring

The material of the ring is 42CrMo alloy steel, and its physical properties and the constitutive equation varying with temperature are provided by PAN [15] and LIN et al [16]. The main features of the FE model are as follows:

1) The rolls are treated as isothermal analytical rigid bodies, and the ring is treated as deformable body which was discretized by the coupled thermo-mechanical hexahedron element with eight nodes (C3D8R).

2) The coupled thermo-mechanical dynamic explicit approach with reasonable mass scaling skill is used to avoid the huge computation time and convergence problem of the implicit procedure, and improve the computation efficiency [17]. The ALE formulation was used to control the mesh distortion [18].

3) The axial constraint is applied to the end surfaces of the ring blank, that is, the axial displacement of the nodes on the end surfaces of the ring blank is not permitted, which can replace the closed rolling pass to limit the axial spread of the ring blank in the actual rolling process.

### 3 Simulation result and discussion

#### 3.1 Evolution and distribution laws of radial spread

A simulation case is performed based on the FE model. One cross-section of the rolled ring is intercepted to analyze the evolution and distribution of the radial spread in the rolling process, as shown in Fig. 5.

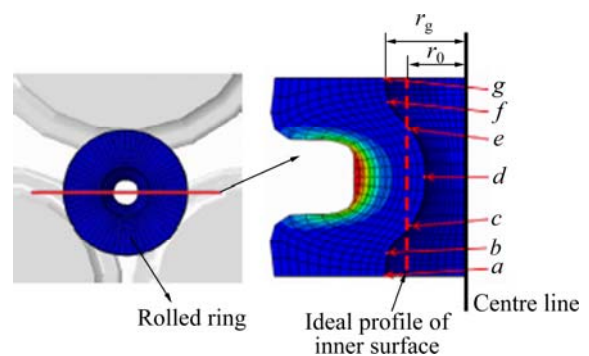


**Fig. 5** Intercepted cross-section and tracing points

In Fig. 5, seven tracing points numbered *a* to *g*, are selected for analysis, which symmetrically distribute around the axial centre. The radial spread of point *g* is defined as

$$\Delta r_g = r_g - r_0 \tag{1}$$

where  $\Delta r_g$  means the radial spread value of point *g*;  $r_g$

means the inner radius at the location of point *g*.

Figure 6 shows the intercepted cross-section varying with increasing the feed amount in the rolling process, it can be seen that the radial spread gradually occurs on the inner surface with the increase of feed amount. Figure 7 indicates that the different axial locations have different variation rules of radial spread. The radial spread variation curves of the two symmetrical tracing points are nearly coincident, including points *a* and *g*, *b* and *f*, *c* and *e*. The radial spread values of points *a*, *b*, *f*, *g* lied in the upper and lower regions increase during the rolling process, while the radial spread values of points *c*, *d*, *e* lied in the axial centre region firstly increase, then decrease in the rolling process.

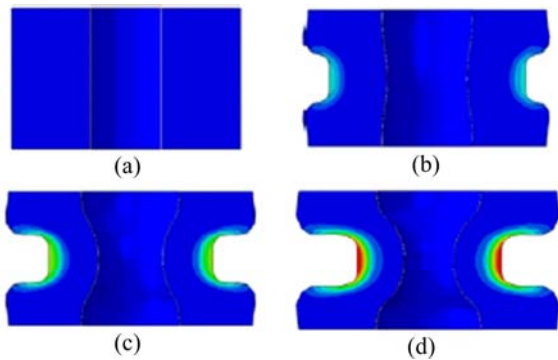


Fig. 6 Cross-section shapes under different feed amounts: (a) 0; (b) 35%; (c) 70%; (d) 100%

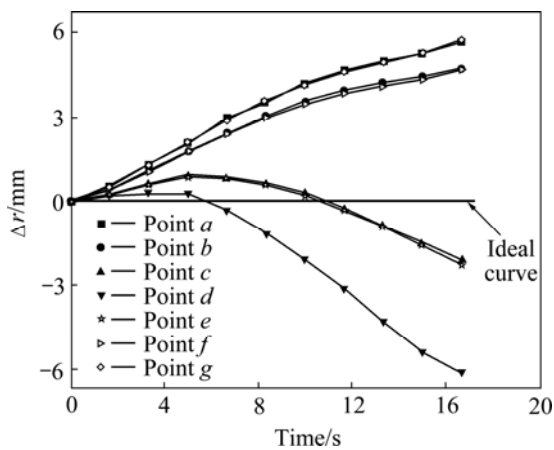


Fig. 7 Radial spread variation curves of seven tracing points in rolling process

The evolution law of radial spread is caused by the different metal flow behaviors in the two forming stages, as shown in Fig. 8. In the initial forming stage, the feed amount is small, the outer surface metal of central region mainly produces axial flow toward to the upper and lower regions, and the outer surface metal of upper and lower region inversely flows to fill the roll cavity. This behavior draws inner surface metal to flow outward, thus

the radial spread of whole inner surface increases. In the following stage, the radial metal flow of central region becomes strong with the increase of feed amount: This pushes the inner surface metal to flow inward, so, the radial spread of the centre region decreases.

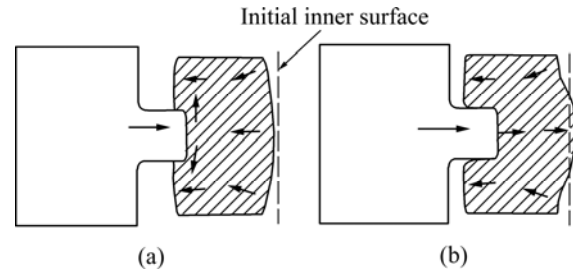


Fig. 8 Metal flow behaviors in two forming stages: (a) Initial stage; (b) Following stage

The radial spread values of the seven tracing points of the rolled ring are provided in Fig. 9. It is shown that the radial spread values decrease from the axial end surfaces to the axial centre, and the radial spread distribution of the inner surface is symmetrical to the axial centre.

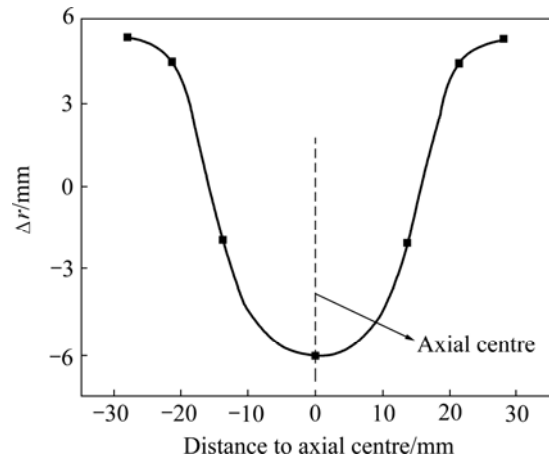


Fig. 9 Radial spread distribution of rolled ring

### 3.2 Influences of key forming parameters

#### 3.2.1 Simulation conditions

The influences of feed velocity *v*, rotational speed *n*, friction coefficient *f* and initial blank temperature *t* on the radial spread were investigated. The simulation conditions are as follows.

Condition 1: To investigate the effect of feed velocity, select  $v=\{1.25, 2.5, 3.75, 5, 6.25, 7\}$ , and the other three parameters keep invariable.

Condition 2: To investigate the effect of rotational speed, select  $n=\{1.78, 2, 2.5, 3.33, 5, 10\}$ , and the other three parameters keep invariable.

Condition 3: To investigate the effect of friction coefficient, select  $f=\{0.25, 0.3, 0.35, 0.4, 0.45, 0.5\}$ , and the other three parameters keep invariable.

Condition 4: To investigate the effect of initial blank temperature, select  $t=\{950, 1050, 1150, 1200, 1250\}^{\circ}\text{C}$ , and the other three parameters keep invariable.

3.2.2 Evaluation index

The average radial spread (ARS) and the inner surface unevenness (ISU) of the rolled ring are employed as the two evaluation indexes, the smaller the ARS and ISU are, the less the radial spread is, and the more flat the inner surface are. ARS and ISU are defined as

$$\text{ARS} = \sum_{i=1}^n \Delta r_i / n \tag{2}$$

$$\text{ISU} = \Delta r_{\max} - \Delta r_{\min} \tag{3}$$

where  $\Delta r_i$  means the radial spread value of node  $i$  from up to down along the inner surface of the intercepted cross-section;  $n$  is the number of the nodes on the inner surface of the intercepted cross-section;  $\Delta r_{\max}$  and  $\Delta r_{\min}$  mean the maximum and minimum radial spread values in the radial spread values of all nodes.

3.2.3 Simulation results

1) Influence of feed velocity

Figure 10 shows the ARS and ISU variation curves with increasing  $v$ . It can be seen that the ARS and ISU both increase with the increase of feed velocity. With the increase of  $v$ , the feed amount per revolution increases, the penetration of deformation zone along the radial direction becomes intensive, which will draw more inner surface metals to attend the metal filling in the first forming stage. And it promotes the inner surface metal to flow inward in the second forming stage. So, the positive radial spread of the axial end region and the negative radial spread of the axial centre region both increase, and the ISU increases. However, in this case, the area of the axial centre region will form as the groove is small than that of the axial end region, thus the increase amount of the positive radial spread is greater than that of the negative radial spread, and the ARS increases.

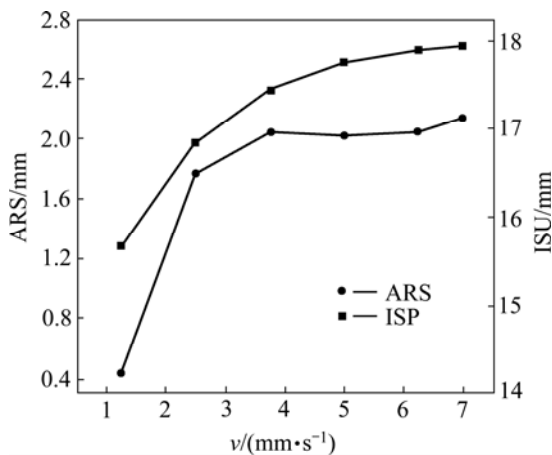


Fig. 10 ARS and ISU variation curves with feed velocity

2) Influence of rotational speed

The ARS and ISU variation curves with increasing  $n$  are provided in Fig. 11. It indicates that the ARS and ISU both decrease with the increase of rotational speed. With the increase of  $n$ , the feed amount per revolution decreases, which has contrary effect on the radial spread behavior compared with the increase of  $v$ , thus the ARS and ISU both decrease.

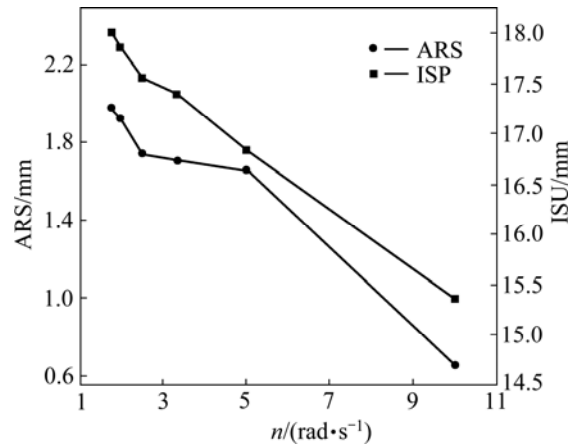


Fig. 11 ARS and ISU variation curves with rotational speed

3) Influence of friction coefficient

Figure 12 shows the ARS and ISU variation curves with increasing  $f$ . It can be seen that ARS decreases and ISU increases with the increase of friction coefficient. With the increase of  $f$ , the heat generation on the outer surface of axial centre region increases by the intensive friction, which will raise the temperature and improve the metal fluidity of outer surface. So, the outer surface metal can flow to the inner surface more easily, and the negative radial spread of the axial centre region increases, the ARS decreases, and ISU increases. It also can be seen that, the variation amplitude of ARS or ISU with the increase of  $f$  is smaller than that with the increase of  $v$  or  $n$ . This indicates that the influence of friction coefficient is slighter than that of feed velocity and rotational speed.

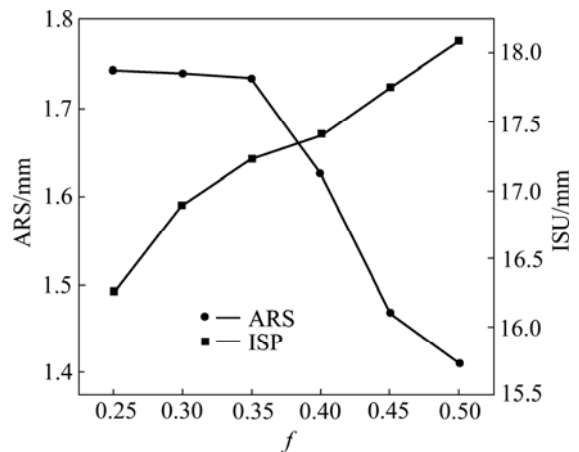


Fig. 12 ARS and ISU variation curves with friction coefficient

#### 4) Influence of initial blank temperature

Figure 13 shows the ARS and ISU variation curves with the increasing temperature. It can be seen that ARS increases and ISU decreases with the increase of initial blank temperature. With the increase of temperature, the metal fluidity of outer surface improves, which promotes the metal flow of outer surface to the inner surface. However, the metal fluidity of inner surface is also enhanced. Thus, the inner surface metal can be drawn to fill the roll cavities more easily, and this metal flow behavior is more prominent. So, the ARS increases and the ISU decreases. It also can be seen that the influence of friction coefficient on radial spread is also slight.

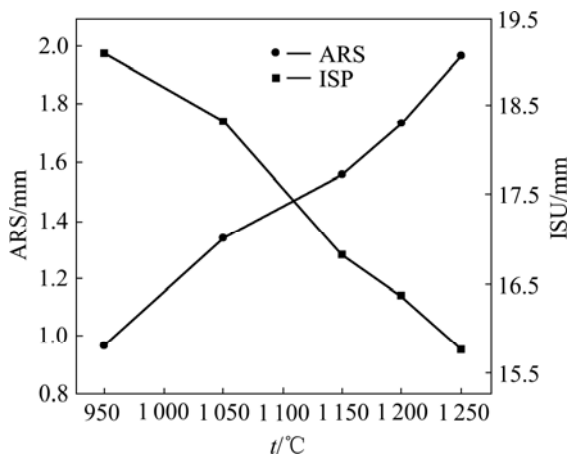


Fig. 13 ARS and ISU variation curves with temperature

## 4 Conclusions

1) During the TRCR process, different regions of the ring inner surface have the different radial spread evolution laws, the radial spread of the central region firstly increases, then decreases, and that of the upper or lower region always increases.

2) The radial spread of the inner surface has a symmetrical distribution along the axial direction after TRCR. It decreases from the upper and lower regions to the middle region. The central region has a negative radial spread, and the upper and lower regions have positive radial spread.

3) A larger feed speed or smaller rotational speed contributes to the larger average radial spread and more unevenness of ring inner surface, and a larger friction coefficient or smaller initial blank temperature contributes to the smaller average radial spread and more unevenness of ring inner surface.

## References

[1] ZHOU Xiu-mei, HUA Lin, QIAN Dong-sheng. 3D FE modelling of three rolls cross rolling process of a rotary disk part [J]. *Advanced*

*Material Research*, 2010, 189–193: 1991–1996.

[2] ZHOU Xiu-mei, HUA Lin, QIAN Dong-sheng. Coupled thermo-mechanical behaviours in symmetric three-roll cross rolling of disk rotary parts [C]// *Proceedings of the 10th International Conference on Technology of Plasticity*. Aachen, 2011: 72–77.

[3] MA Qi, HUA Lin, QIAN Dong-sheng. Coupled thermo-mechanical FEA of three-roll cross rolling process for rings with small-hole and deep groove [J]. *Advanced Materials Research*, 2012, 560–561: 846–852.

[4] SONG J L, DOWSON A L, JACOBS A M H, BROOKS J, BEDEN I. Coupled thermo-mechanical finite-element modeling of hot ring rolling process [J]. *Journal of Materials Processing Technology*, 2002, 121: 332–340.

[5] WANG Min, YANG He, SUN Zhi-chao, GUO Liang-gang. Dynamic explicit FE modeling of hot ring rolling process [J]. *Transactions of Nonferrous Metals Society of China*, 2006, 16(6): 1274–1280.

[6] WANG Min. comparison of evolution laws of stress and strain fields in hot rolling of titanium alloy large rings with different sizes [J]. *Transactions of Nonferrous Metals Society of China*, 2011, 21(7): 1611–1619.

[7] KIM K H, SUK H G, HUB M Y. Development of the profile ring rolling process for large slewing rings of alloy steels [J]. *Journal of Materials Processing Technology*, 2007, 187–188: 730–733.

[8] SUN Zhi-chao, YANG He, OU Xin-zhe. Thermo-mechanical coupled analysis of hot ring rolling process [J]. *Transactions of Nonferrous Metals Society of China*, 2008, 18(5): 1216–1222.

[9] WANG Z W, ZENG S Q, YANG X H, CHENG C. The key technology and realization of virtual ring rolling [J]. *Journal of Materials Processing Technology*, 2007, 182(1–3): 374–381.

[10] WANG Z W, FAN J P, HU D P, TANG C Y, TSUI C P. Complete modeling and parameter optimization for virtual ring rolling [J]. *International Journal of Mechanical Sciences*, 2010, 52(10): 1325–1333.

[11] HUA Lin, PAN Li-bo, LAN Jian. Researches on the ring stiffness condition in radial-axial ring rolling [J]. *Journal of Materials Processing Technology*, 2009, 209(5): 2570–2575.

[12] ZHOU Guang, HUA Lin., LAN Jian. 3D coupled thermo-mechanical FE modeling and simulation of radial-axial ring rolling [J]. *Materials Research Innovations*, 2011, 15(S1): 221–224.

[13] ZHOU Guang, HUA Lin, LAN Jian, QIAN Dong-sheng. FE analysis of coupled thermo-mechanical behaviors in radial-axial rolling of alloy steel large ring [J]. *Computational Materials Science*, 2010, 50(1): 65–76.

[14] GUO Liang-gang, YANG He. Towards a steady forming condition for radial-axial ring rolling [J]. *International Journal of Mechanical Sciences*, 2011, 53(4): 286–299.

[15] PAN Jia-zhen. *Pressure vessel material practical manual* [M]. Beijing: Chemical Industry Press, 2000. (in Chinese)

[16] LIN Yong-cheng, CHEN Ming-song, ZHONG Jue. Constitutive modelling for elevated temperature flow behaviour of 42CrMo steel [J]. *Computational Materials Science*, 2008, 42(3): 470–477.

[17] GUO Liang-gang, YANG He, ZHAN Mei. Research on the plastic deformation behaviour in cold ring rolling by FEM numerical simulation [J]. *Modelling and Simulation in Material Science and Engineering*, 2005, 13(7): 1029–1046.

[18] DAVEY K, WARD M J. A practical method for finite element ring rolling simulation using the ALE flow formulation [J]. *International Journal of Mechanical Science*, 2002, 44(1): 165–190.

# 小孔深槽环件三辊横轧径向宽展行为的有限元分析

钱东升<sup>1</sup>, 华林<sup>1,2</sup>, 邓加东<sup>1</sup>

1. 武汉理工大学 材料科学与工程学院, 武汉 430070;
2. 武汉理工大学 现代汽车零部件技术湖北重点实验室, 武汉 430070

**摘 要:** 为了更好地理解径向宽展行为并提出有效的控制方法, 利用 ABAQUS\ Explicit 开展深槽小孔环件三辊横轧径向宽展行为的有限元分析, 研究三辊横轧过程中径向宽展演化和分布规律、以及 4 个关键成形参数对径向宽展行为的影响规律。结果表明: 三辊横轧中环件内表面中心区域径向宽展先增加后减小, 上、下区域一直增加; 三辊横轧后径向宽展关于轴向中心呈对称分布, 从上、下区域至中心区域逐渐减小; 较大的进给速度或较小的转速会导致较大的平均宽展和内表面不平整度; 较大的摩擦系数或较小的环件初始温度会导致较小的平均宽展和较大的内表面不平整度。该结果能够为深槽小孔环件三辊横轧径向宽展控制和合理的参数设计提供科学依据。

**关键词:** 三辊横轧; 小孔深槽环件; 径向宽展; 有限元分析; 回转成形; 塑性变形

(Edited by LI Xiang-qun)